Simulations of the Lunar Photoelectron Sheath and Associated Dust Grain Levitation Equilibria

A. Poppe and M. Horányi

Laboratory for Atmospheric and Space Physics (LASP), Boulder, CO

Dept. of Physics, University of Colorado, Boulder, CO

LPSC 2010

Session 611 - #1218

Work supported by the NASA Earth and Space Science Graduate Fellowship Program (Grant #NNX08BA17H) and the Colorado Center for Lunar Dust and Atmospheric Studies of the NASA Lunar Science Institute

Abstract

Previous observations have identified a number of phenomena on the lunar surface that are best explained as results of dusty plasma processes leading to dust charging, levitation and horizontal transport. These observations include Surveyor images of Horizon Glow (HG), astronaut sketches of dust streamers and in-situ measurements made by the Lunar Ejecta and Meteorites (LEAM) experiment. Recent laboratory experiments that approximately reproduced the near surface lunar plasma environment showed that charging can lead to the levitation and transport of dust grains in a tenuous electron sheath. A critical ingredient to the observed phenomena is the presence of a photoelectron sheath, formed when solar ultraviolet radiation causes the lunar regolith to emit electrons. In order to understand the dynamics and underlying physics of dust particles on the surface of the Moon, the lunar photoelectron sheath has been modeled via a 1-dimensional particle-in-cell (PIC) code. In order to validate this code, the results are compared with analytical solutions of the electron density, electric field and sheath thickness for three standard electron velocity distributions. Post-validation, initial simulations have focused on the dependence of the lunar photoelectric sheath on non-standard electron velocity distributions and an incoming solar wind flux. Further additions to the model will include the temporal evolution of the solar UV flux and the presence of dust particles, especially their role as sources and sinks of plasma.

Motivation

Apollo-era observations have suggested the possibility of electrostatically levitated dust grains above the lunar surface. These observations include measurements by the Lunar Ejecta and Meteorites experiment [1], shown in **Figure 1**, and Surveyor images of lunar Horizon Glow [2], shown in **Figure 2**. The LEAM results were interpreted as highly-charged, slowly-moving dust grains that were electrostatically transported across the lunar surface and the Surveyor images were explained as forward-scattered sunlight by levitated dust particles. Additionally, recent laboratory experiments have demonstrated the ability to charge and levitate grains in a plasma [3-6]. The lunar surface is exposed to a number of plasma processes, including photoemission from solar UV radiation and collection of ambient solar wind electrons and ions, depicted in **Figure 3**. In order to fully explain these phenomena, an understanding of the lunar surface plasma environment is required.

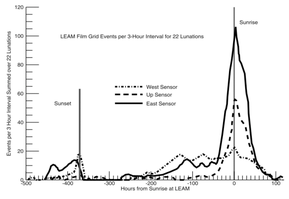

Figure 1: LEAM Observations [1]

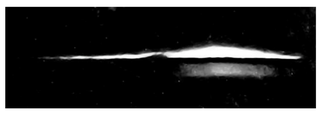

Figure 2: Surveyor image of lunar Horizon Glow [2].

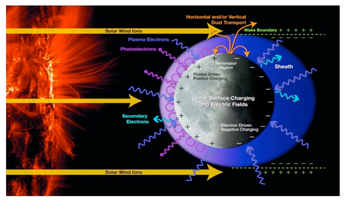

Figure 3: Plasma environment at the Moon

Simulation

In order to simulate the lunar photoelectron sheath, we have developed a 1-dimensional particle-in-cell code, following the standard outline in [7]. Photoelectrons are emitted from the lunar surface on the left side of the simulation, while solar wind ions and electrons enter the simulation from vacuum on the right. Two velocity distributions for the photoelectrons are studied: the measured velocity distribution from [8], modeled as $v^4 e^{-v^4/v_e^4}$, and a T_e=*2.2* eV Maxwellian, for comparison. The solar wind is modeled as a quasi-neutral, T_{sw}=*10* eV Maxwellian with a 400 km/sec drift speed. The net surface charge on the lunar surface is continuously calculated to maintain charge conservation. The simulation was able to successfully reproduce an analytic derivation of a simple photoelectron sheath [9], and therefore, can be applied to further simulations with confidence.

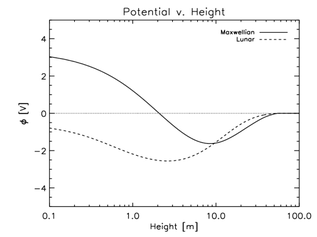

Figure 1: Sheath potential as a function of height for both the lunar and Maxwellian cases.

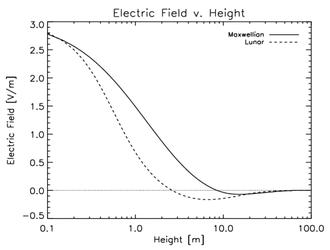

Figure 2: Sheath electric field profile for both the lunar and Maxwellian cases. Note the regions of negative electric field for both cases.

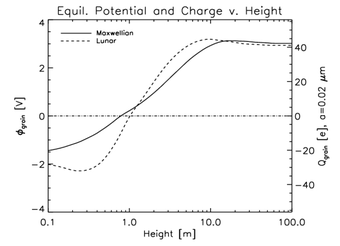

Figure 3: Equilibrium grain potential and charge for both the lunar and Maxwellian cases.

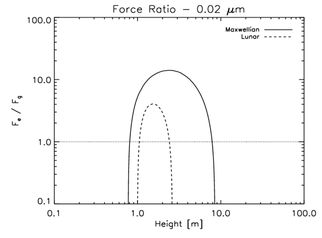

Figure 4: Grain force ratio as a function of height above the lunar surface.

Results

I. Sheath Profiles

For the Maxwellian case, we find at the surface an electron density of $n_e = 1.5 \cdot 10^8$ m^{-3}, Debye length, λ_D = 1.0 m, and electric field, E_o = 2.8 V/m, while for the lunar case, the parameters are $n_e = 1.3 \cdot 10^8$ m^{-3}, λ_D= 1.1 m and E_o = 2.8 V/m. While the two different cases, Maxwellian and lunar, have similar plasma parameters, they differ in their potential and electric field profiles. As shown in **Figure 1**, both cases were found to have non-monotonic potential distributions, a situation which has been previously analyzed from a theoretical perspective [10]. Shown in **Figure 2** is a comparison of the electric field above the surface for the lunar and Maxwellian photoelectron emission distributions. The electric field in the lunar photoelectron sheath is weaker than the field in the Maxwellian sheath. Additionally, due to the non-monotonicity of the potential, both cases have regions of negative, or downward-pointing, electric field. By ~50 m above the surface, the sheath dies out and the plasma returns to its background, quasi-neutral state of the solar wind. This detailed knowledge of the lunar plasma environment will allow a more accurate investigation of dusty phenomena near the lunar surface.

II. Grain Charging and Equilibria

To study the characteristics of electrostatically levitated dust grains on the lunar surface, we employ a test-particle method for dust grains embedded in the sheath. A grain immersed in a plasma will reach the potential at which the charging currents to the grain sum to zero. Using the capacitance of a spherical grain, the grain charge can be calculated as $Q = 4\pi\varepsilon_o r V$, where r is the grain radius and V is the grain potential. **Figure 3** shows the equilibrium grain potential and charge for a 0.02 μm grain as a function of height above the lunar surface. The Maxwellian and lunar curves have qualitatively similar shapes, with the particle reaching ~5 V in the solar wind.

A charged dust grain will levitate in a photoelectron sheath if the electric and gravitational forces on the grain balance. Using the grain charge from **Figure 3** and the electric field profile from **Figure 2**, the ratio of the electric to gravitational force on the grain can be calculated. Shown in **Figure 4** is the force ratio for a 0.02 μm grain as a function of height. The lunar case has a consistently lower force ratio, mainly due to the weaker lunar electric field. For this particle size, the grain will levitate at ~2.5 m and ~8.5 m for the lunar and Maxwellian cases, respectively.

The equilibrium levitation height can be found for all particles sizes and is shown in **Figure 5.** The levitation height for the Maxwellian case is consistently higher that of the lunar case. For the Maxwellian case, the maximum levitation height and size are 8.5 m and ~0.15 μm, respectively, while for the lunar case, 2.5 m and ~0.085 μm. The relative inability of the lunar sheath to levitate dust grains stems mainly from the relatively weaker electric field through the sheath.

III. Solar UV Variability

Increased photoemission due to solar maximum and solar flare conditions increases the sheath electric field and also causes grains to attain a higher charge throughout the sheath. These two effects increase the ability of the sheath to levitate dust grains. **Figure 6** shows the equilibrium grain potential and charge for a 0.02 μm grain for the solar minimum, solar maximum and solar flare conditions. The maximum charge on a 0.02 μm grain increases from ~40 e during solar minimum to ~70 e and ~90 e during solar maximum and solar flare conditions, respectively. Additionally, the height at which the grain potential and charge transition from negative to positive occurs at successively lower heights for increased photoemission.

Using the same analysis as Section II, the force ratio as a function of height and the equilibrium levitation height as a function of grain radius can be determined for the solar maximum and solar flare conditions. In **Figure 7**, an increase in the ratio of the electric to gravitational forces on a 0.02 μm grain for both the solar maximum and solar flare conditions is shown. For example, at 1 m, the force ratio for the 0.02 μm grain increase by factors of 10- and 20-fold for the solar maximum and solar flare conditions, respectively. The increase is due to the combination of the increase in the sheath electric field and the increase in the equilibrium grain charge. **Figure 8** shows the equilibrium levitation height as a function of grain radius for all three solar UV conditions. The maximum grain radius that can be levitated increases from 0.04 μm for solar minimum conditions, to 0.075 μm and 0.12 μm for solar maximum and flare conditions, respectively. Additionally, the maximum levitation height decreases for increasing solar irradiation, due to the decreasing height of the point at which the sheath electric field becomes negative.

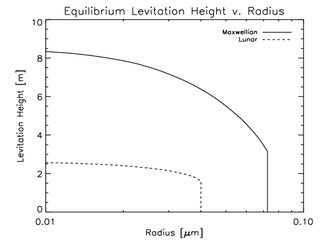

Figure 5: Equilibrium levitation height

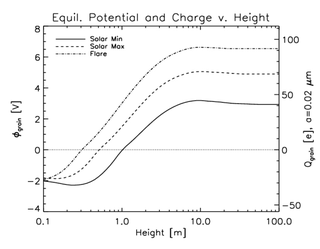

Figure 6: Equilibrium grain potential and charge with UV variability

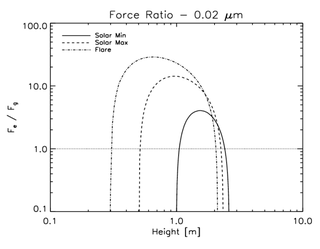

Figure 7: Equilibrium force ratio with UV variability

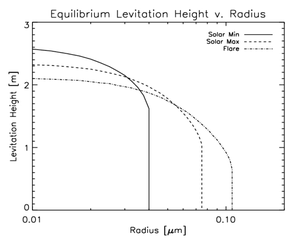

Figure 8: Equilibrium levitation height with UV variability

[1] O. Berg *et al.*, Geo. Res. Lett., **1**, 1974
[2] J. Rennilson and D. Criswell, The Moon, **10**, 1973
[3] Sickafoose, A. *et al.*, Phys. Rev. Lett., **84**, 2000
[4] Sickafoose, A. *et al.*, J. Geo. Res., **106**, 2001
[5] Wang, X. *et al.*, Geo. Res. Lett., **34**, 2007
[6] Wang, X. *et al.*, J. Geo. Res., **114**, 2009
[7] Birdsall, C. K. and A. B. Langdon, McGraw Hill, 1984
[8] Feuerbacher, B. *et al.*, Proc. 3rd Lun. Sci. Conf., **3**, 1972
[9] Grard, R. J. L. and J. K. E. Tunaley, J. Geo. Res., **76**, 1971
[10] Guernsey, R. L. and H.J.M. Fu, J. Geo. Res., **75**, 1970